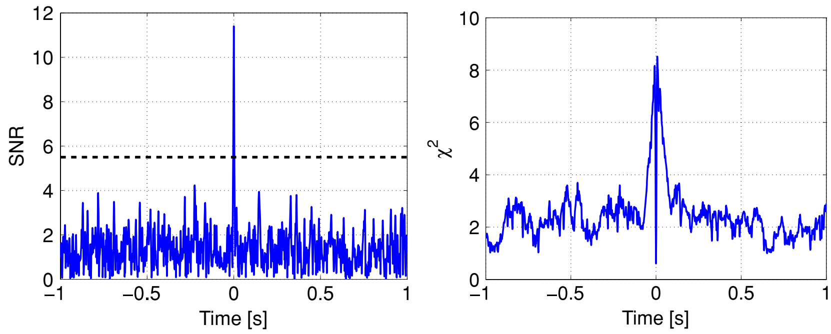

Figure 7. SNR (left) and χ^2 (right) [8, 9] time series obtained after match-filtering the Livingston data containing the *Candidate G* (simulated inspiral gravitational-wave signal). The time origin on the x-axis coincides with the time of the inspiral trigger. In the left plot the dashed horizontal line at SNR = 5.5 corresponds to the SNR threshold used for this analysis. SNR peaks exceeding this threshold are recorded as inspiral triggers by the analysis pipeline. In the right plot, the χ^2 time series shows a characteristic pattern for a few tens of milliseconds around the time of the *Candidate G* ($t = 0$ s) which corresponds to the expectations for a gravitational-wave signal. In particular, the χ^2 is minimum at $t = 0$ s when the triggered waveform best matches the signal present in the data.

with time) that is characteristic of an inspiral signal. The simulated gravitational-wave signal is thus visible in these two spectrograms. It is actually not clearly visible in the *Q spectrogram* of the H2 data (not represented here) because of the lower SNR in this interferometer.

4.3.2. Output of the match-filtering algorithm. Another example of check for the candidate's appearance that is used by the CBC group consists in examining the time series of the SNR obtained after match-filtering [9] the data with inspiral waveforms [14], as well as the time series of a χ^2 which tests the consistency between the triggered waveform and the signal present in the data.

An example of the expected time series for a simulated gravitational-wave signal is shown in figure 7. In the left plot, the SNR time series shows a short central peak exceeding the threshold at SNR = 5.5 used by this search. This SNR peak corresponds to the time of the trigger associated with the simulated inspiral signal. In the right plot, the χ^2 time series presents a very characteristic shape around the time of the inspiral trigger ($t = 0$ s), which corresponds to the expectations for gravitational-wave signal in stationary Gaussian noise. A few milliseconds before the time of the inspiral trigger the χ^2 value starts increasing, while it falls to a minimum at $t = 0$ s when the triggered waveform best matches the simulated gravitational-wave signal injected in the data. Finally the χ^2 time series presents a symmetrical behaviour after $t = 0$ s.

Note that a veto based on the value of the χ^2 at the time of the inspiral trigger (which would correspond to $t = 0$ s in figure 7) is already automatically implemented in the CBC analysis pipeline. This veto rejects any trigger whose χ^2 value exceeds a threshold set to $\chi^2 = 10$ in the search that identified *Candidate G* and *Candidate F*. The tuning of this threshold tends to be very conservative to assure that real gravitational-wave events with waveforms that might differ slightly from the CBC search templates are not rejected [30]. The qualitative check performed in the detection checklist is complementary to the χ^2 veto as it consists in examining the χ^2 time series for several tenths of seconds around the inspiral trigger.

Figure 8 shows the SNR and χ^2 time series around the time of the *Candidate F* at Livingston. Multiple peaks of SNR exceeding the threshold are visible in the left plot, which

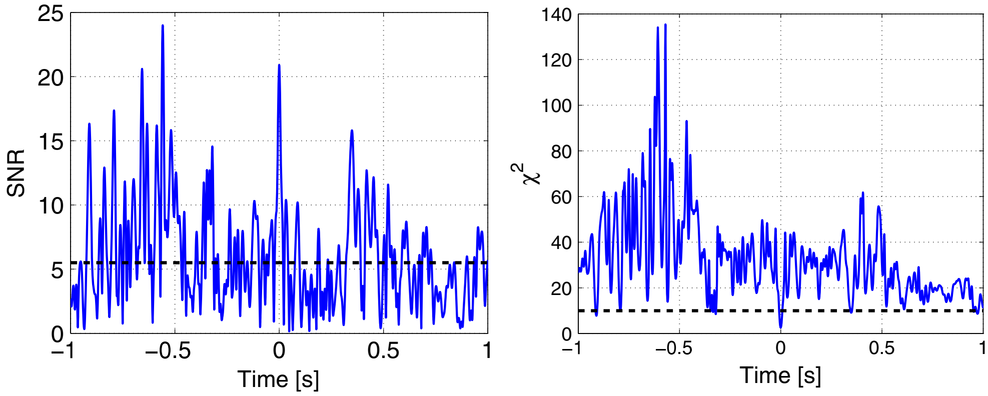

Figure 8. SNR (left) and χ^2 (right) [8, 9] time series obtained after match-filtering the Livingston data containing the *Candidate F* (false alarm). The time origin on the *x*-axis coincides with the time of the inspiral trigger. In the left plot the dashed horizontal line at SNR = 5.5 corresponds to the SNR threshold, while, in the right plot, the dashed horizontal line at $\chi^2 = 10$ corresponds to the χ^2 threshold used for this analysis. The inspiral triggers must exceed the SNR threshold while their χ^2 must be lower than the corresponding threshold.

indicates highly non-stationary data. In the right plot the χ^2 time series does present a minimum at $t = 0$ s which is the reason why this candidate was not vetoed by the analysis pipeline. However the χ^2 time series also shows large values for the whole two seconds window surrounding the candidate, which clearly differs from the plot shown in figure 7 and indicates a very noisy stretch of data. Accordingly the *Candidate F* can be ruled out as a possible detection, which confirms the first suspicions born from the analysis of the *inspiral range* in section 4.1.

5. Conclusions and perspectives

The Burst and CBC groups are pursuing the refinement of their respective detection checklists for candidate-event validation. Part of these tests are still under development and are expected to become more quantitative as experience about the instruments is gained. The groups are currently aiming to automate the detection checklist in order to build a candidate follow-up pipeline which will improve the swiftness of the analysis. The detection checklist is presently being applied to the candidates obtained by the searches analysing the data taken during the fifth LIGO science run (S5) [1]. The detection checklist should play an even more crucial role in the analysis of the future LIGO science runs, for which we expect better detectors' sensitivities and higher probabilities of gravitational-wave detections.

Acknowledgments

The authors gratefully acknowledge the support of the United States National Science Foundation for the construction and operation of the LIGO Laboratory and the Science and Technology Facilities Council of the United Kingdom, the Max-Planck-Society and the State of Niedersachsen/Germany for support of the construction and operation of the GEO600 detector. The authors also gratefully acknowledge the support of the research by these agencies and by the Australian Research Council, the Council of Scientific and Industrial

Research of India, the Istituto Nazionale di Fisica Nucleare of Italy, the Spanish Ministerio de Educación y Ciencia, the Conselleria d'Economia, Hisenda i Innovació of the Govern de les Illes Balears, the Scottish Funding Council, the Scottish Universities Physics Alliance, The National Aeronautics and Space Administration, the Carnegie Trust, the Leverhulme Trust, the David and Lucile Packard Foundation, the Research Corporation and the Alfred P Sloan Foundation. This work has also been supported by NFS award PHY0605496 and PHY0355289. This paper was assigned LIGO document number LIGO-P080042-05-Z.

References

[1] Abbott B *et al* (LIGO Scientific Collaboration) 2007 LIGO: the laser interferometer gravitational-wave observatory *Preprint* arXiv:0711.3041
[2] Acernese F *et al* (Virgo Collaboration) 2007 *Class. Quantum Grav.* **24** S381–88
[3] Thorne K S 1987 *300 years of Gravitation* ed S W Hawking and W Israel (Cambridge: Cambridge University Press) p 330
[4] Blanchet L, Damour T, Iyer B R, Will C M and Wiseman A G 1995 *Phys. Rev. Lett.* **74** 3515–18
[5] Pradier T, Arnaud N, Bizouard M-A, Cavalier F, Davier M and Hello P 2000 *Int. J. Mod. Phys.* D **9** 309–14 (*Preprint* gr-qc/0001062)
[6] Zivkovic I and Weinstein A 2001 *Tech. Rep.* LIGO-T010157-00 LIGO Project http://www.ligo.caltech.edu/docs/T/T010157-00.pdf
[7] Blackburn L *et al* 2008 The LSC glitch group: monitoring noise transients during the 5th LIGO science run *Class. Quantum Grav.* **25** 184004 (*Preprint* arXiv:0804.0800)
[8] Allen B 2005 *Phys. Rev.* D **71** 062001
[9] Allen B, Anderson W G, Brady P R, Brown D A and Creighton J D E 2005 FINDCHIRP: an algorithm for detection of gravitational waves from inspiraling compact binaries *Preprint* gr-qc/0509116
[10] McNabb J W C, Ashley M, Finn L S, Rotthoff E, Stuver A, Summerscales T, Sutton P, Tibbits M, Thorne K and Zaleski K 2004 *Class. Quantum Grav.* **21** S1705–10 (*Preprint* gr-qc/0404123)
[11] Chatterji S, Blackburn L, Martin G and Katsavounidis E 2004 *Class. Quantum Grav.* **21** S1809–18
[12] Chatterji S 2005 *PhD Thesis*, Massachusetts Institute of Technology http://hdl.handle.net/1721.1/34388
[13] Klimenko S and Mitselmakher G 2004 *Class. Quantum Grav.* **21** S1819–30
[14] Blanchet L, Iyer B, Will C M and Wiseman A G 1996 *Class. Quantum Grav.* **13** 575
[15] Röver C, Meyer R and Christensen N 2006 *Class. Quantum Grav.* **23** 4895–906
[16] Landry M (for the LIGO Scientific Collaboration) 2005 *Class. Quantum Grav.* **22** S985–94
[17] Siemens X, Allen B, Creighton J, Hewitson M and Landry M 2004 *Class. Quantum Grav.* **21** S1723–36 (*Preprint* gr-qc/0405070)
[18] Lück H *et al* 2006 *Class. Quantum Grav.* **23** S71–78
[19] Abbott B *et al* (LIGO Scientific Collaboration and Virgo Collaboration) 2008 *Class. Quantum Grav.* **25** 114051
[20] Klimenko S, Mohanty S, Rakhmanov M and Mitselmakher G 2005 *Phys. Rev.* D **72** 122002
[21] Mercer R A and Klimenko S 2008 Visualising GW event candidates using the coherent event display *Class. Quantum Grav.* **25** 184025
[22] Bose S, Pai A and Dhurandhar S V 2000 *Int. J. Mod. Phys.* D **9** 325–29 (*Preprint* gr-qc/0002010)
[23] Pai A, Dhurandhar S and Bose S 2001 *Phys. Rev.* D **64** 042004 (*Preprint* gr-qc/0009078)
[24] Guersel Y and Tinto M 1989 *Phys. Rev.* D **40** 3884
[25] Röver C, Meyer R and Christensen N 2007 *Phys. Rev.* D **75** 062004
[26] Baggio L *et al* (AURIGA Collaboration and LIGO Scientific Collaboration) 2008 *Class. Quantum Grav.* **25** 095004 (*Preprint* arXiv:0710.0497)
[27] Abbott B *et al* (LIGO Scientific Collaboration) 2008 *Phys. Rev.* D **77** 062002
[28] Finn L S and Chernoff D F 1993 *Phys. Rev.* D **47** 2198
[29] Schofield R 2008 Environmental coupling during S5, LIGO-G080209-00 LIGO Project http://www.ligo.caltech.edu/docs/G/G080209-00/G080209-00.pdf
[30] The LIGO Scientific Collaboration 2007 Tuning matched filter searches for compact binary coalescence, LIGO-T070109-01 LIGO Project http://www.ligo.caltech.edu/docs/T/T070109-01.pdf